https://doi.org/10.5194/egusphere-2024-1055
Preprint. Discussion started: 11 April 2024

Expanding seawater carbon dioxide and methane measuring capabilities with a Seaglider

Claudine Hauri[1*], Brita Irving[1], Dan Hayes[2], Ehsan Abdi[3,4], Jöran Kemme[5], Nadja Kinski[5], and Andrew M. P. McDonnell1[6,7]

[1]International Arctic Research Center, University of Alaska Fairbanks, Fairbanks, AK 99775, USA

[2]Advanced Offshore Operations, Inc., Houston, TX 77004, USA

[3]Cyprus Subsea Consulting and Services, Lakatamia 2326, Cyprus

[4]now at Akvaplan-Niva, 9296 Tromsø, Norway

[5] -4H-JENA engineering GmbH, 07745 Jena, Germany

[6] College of Fisheries and Ocean Science, University of Alaska Fairbanks, Fairbanks, AK 99775, USA

[7]now at Alaska Renewables, Fairbanks, AK 99709, USA

Corresponding author: Claudine Hauri (chauri@alaska.edu)

https://doi.org/10.5194/egusphere-2024-1055
Preprint. Discussion started: 11 April 2024

Abstract

Warming, ocean acidification, and deoxygenation are increasingly putting pressure on marine ecosystems. At the same time, thawing permafrost and decomposing hydrates in Arctic shelf seas may release large amounts of methane (CH_4) into the water column, which could accelerate local ocean acidification and contribute to climate change. The key parameters to observing and understanding these complex processes and feedback mechanisms are vastly undersampled throughout the oceans. We developed carbon dioxide (CO_2) and CH_4 gliders, including standard operational procedures with the goal that CO_2 and CH_4 measurements become more common for glider operations. The Seagliders with integrated Contros HydroC CO_2 or CH_4 sensors also include conductivity, temperature, depth, oxygen, chlorophyll-a, backscatter, and fluorescent dissolved organic matter sensors. Communication via satellite allows for near-real time data transmission, sensor adjustments, and adaptive sampling. Several sea trials with the CO_2 Seaglider in the Gulf of Alaska and data evaluation with discrete water and underway samples suggest near 'weather quality' CO_2 data as defined by the Global Ocean Acidification Network. A winter mission in Resurrection Bay, Alaska provides first insights into the water column inorganic carbon dynamics during this otherwise undersampled season. The CH_4 Seaglider passed its flight trials in Resurrection Bay and is ready to be deployed in an area with greater CH_4 activity. Both sensing systems are available to the science community through the industry partners (Advanced Offshore Operations and -4H-JENA) of this project.

1. Introduction

The oceanic reservoir of carbon dioxide (CO_2) is large, dynamic, spatially variable, and of critical importance to Earth's climate, biogeochemical cycles, and the health of marine

https://doi.org/10.5194/egusphere-2024-1055
Preprint. Discussion started: 11 April 2024

ecosystems. Within the ocean, CO_2 levels (measured as the partial pressure of CO_2, pCO_2) are spatially and temporally variable as they are influenced by a myriad of highly dynamic physical, chemical, and biological processes. On top of this natural variability, the ocean has absorbed about one third of the CO_2 emitted by humans since the industrial revolution (Sabine et al., 2004; Gruber et al., 2019). In doing so, it has played an important role in mitigating climate change (Sabine and Tanhua, 2010). However, both the oceanic uptake of anthropogenic CO_2 and climate change are altering the distribution of oceanic CO_2 and are causing ocean acidification (Doney et al., 2009; Qi et al., 2022; Woosley and Millero, 2020). At the same time, the oceans are warming and losing oxygen (Johnson and Lyman, 2020; Breitburg et al., 2018), increasing the stress on marine ecosystems. As these long-term changes unfold, marine heat waves, and high acidity or low oxygen extreme events will last longer, become more intense, and happen more often and at the same time (Laufkötter et al., 2020; Gruber et al., 2021; Hauri et al., 2024). Negative effects on certain organisms are even stronger if exposed to a combination of different stressors (Breitberg et al., 2015; Kroeker et al., 2017). Positive feedback mechanisms, like warming induced CH_4 seepage from destabilizing hydrates and thawing subsea permafrost, may further accelerate ocean acidification and climate change (Garcia-Tigreros et al., 2021; Sparrow et al., 2018; Shakhova et al., 2010; Rees et al., 2022).

The key parameters to observing and understanding these complex processes and feedback mechanisms are vastly undersampled throughout the oceans owing to conventional sampling approaches that rely primarily on discrete water sample collections from dedicated research cruises, underway measurements of surface ocean properties from transiting vessels, or time series measurements from in situ sensors on fixed moorings. Biogeochemical sensors deployed on autonomous platforms have become more commonly used but power requirements,

https://doi.org/10.5194/egusphere-2024-1055
Preprint. Discussion started: 11 April 2024

long conditioning periods, sensor stability, drift, size, data quality, biofouling, and the need for discrete sample validation and calibration in the field continue to present significant obstacles to widespread adoption and utilization. Autonomous and spatially highly resolved surface measurements of pCO_2 and pH are collected with wave gliders and sail drones (Chavez et al., 2018; Nickford et al., 2022; Manley and Willcox, 2010). Biogeochemical Argo floats are the state of the art autonomous platform to measure a subset of these variables, including pH, O_2, NO_3, chlorophyll-*a*, suspended particles, and downwelling irradiance in subsurface waters (Claustre et al., 2020). BGC Argo floats can last for several years at low sampling resolution, e.g. a 2000 m depth profile every ten days, or they can be programmed for high resolution and shallow sampling as well. The floats can also sample underneath seasonal sea ice (Briggs et al., 2018). However, their trajectory cannot be easily manipulated, and they are not typically recovered at the end of their mission, which prevents sensor calibration and post-mission corrections.

Ocean gliders autonomously collect water column data along planned waypoints, which allows for controlled exploration and adaptive sampling. A variety of pH sensors have been integrated into ocean gliders (Hemming et al., 2017; Saba et al., 2019; Possenti et al., 2021; Takeshita et al., 2021), with the most promising results from ISFET based pH sensors (Saba et al., 2019; Wright-Fairbanks et al., 2020; Takeshita et al., 2021). However, ISFET based pH sensors require significant conditioning periods prior to deployment, suffer from biofouling, require annual cleaning and calibration at the manufacturer, as well as careful discrete sample collection at deployment and recovery to characterize and correct for sensor drift (Thompson et al., 2021). There have been few attempts to integrate pCO_2 sensors into gliders (Hemming et al., 2017; Hauri et al., 2018; von Oppeln-Bronikowski et al., 2021). Hemming et al. (2017) did not

https://doi.org/10.5194/egusphere-2024-1055
Preprint. Discussion started: 11 April 2024

publish the data because quality was so low. Von Oppeln-Bronikowski et al. (2021) integrated an Aanderaa CO_2 optode that measures pCO_2 through detecting the luminescent quenching response from a CO_2-sensitive membrane with a Slocum G2 glider but suffered from instability, thermal-lag issues, variable conditioning periods (4 days to 1 month), large offsets (> 1000 uatm), nonlinear temperature-dependent response time, and a high dependence on prior foil calibration. The highest quality CO_2 sensors rely on membrane equilibration and NDIR spectrometry. Hauri et al. (2018) integrated the Pro Oceanus Mini Pro CO_2 sensor with a Slocum G2. However, the Pro Oceanus Mini Pro CO_2 sensor used at the time did not withstand the pressure changes imposed by glider missions. The Franatech METS CH_4 sensor has been integrated into Alseamar SeaExplorer and Teledyne Slocum gliders and successfully used to generate concentration maps of a methane seep in a semi-quantitative way (Meurer et al., 2021).

Here we integrated modified versions of the Contros HydroC CO_2 and CH_4 sensors with a Seaglider® (registered trademark of the University of Washington). We discuss details of the physical and software integration, present CO_2 and CH_4 data from tank experiments, evaluate the quality of pCO_2 data collected during CO_2 Seaglider missions, and discuss highlights from missions in Resurrection Bay, Alaska.

2. Methods

2.1 CO_2 Seaglider

We integrated a modified version (Seaglider (SG) HydroC CO_2) of the CONTROS HydroC™ CO_2 sensor (-4H-JENA Engineering GmbH, Kiel, Germany) with a Seaglider M1 (Figure 1 a and b). The Seaglider M1 is specifically designed for long endurance missions in deep waters to 1000 m depth. The HydroC CO_2 sensor has a semi-permeable TOUGH membrane

https://doi.org/10.5194/egusphere-2024-1055
Preprint. Discussion started: 11 April 2024

(Pinnau and Toy, 1996) that equilibrates dissolved CO_2 between the ambient seawater and the headspace of the sensor, where the gas concentration is determined by nondispersive infrared (NDIR) spectrometry. The sensor has a zero-signal function (Fietzek et al., 2014), which allows for post mission correction of potential instrument drift and determination of in situ sensor response time. More technical details about the sensor and its performance are described in Fietzek et al., (2014). Since the equilibration time (response time) of membrane-based sensors is affected by the exchange of the water mass in front of the sensor head, we installed a Seabird Electronics (SBE) 5M pump next to the SG HydroC CO_2 sensor using tubing to transfer seawater from outside the glider fairing to the membrane surface (Figure 1a). The response time was determined at the manufacturer, verified in the field and then used to correct for hysteresis during the post-processing phase (see section 2.7.2).

The form factor of the HydroC CO_2^{TM} sensor and Seaglider were changed to achieve an internal integration of the sensor with the Seaglider. The standard high performance HydroC CO_2^{TM} sensor was changed from ⌀ 89 x 380 mm to ⌀ 136 x 294 mm by rearranging the gas-cycle components and the control unit (Figure 1c). This new SG HydroC CO_2 sensor is available in POM cladding rated to 300 m or a titanium housing rated to 1000 m to provide a choice between a coastal mission and an offshore deeper mission. Use of the titanium housing requires a syntactic foam housing to compensate for the weight, whereas the POM housing can be integrated into the glider with simple brackets (Figure 2). Despite these adjustments to the size of the sensor, to our knowledge it is still the largest and heaviest sensor that has been integrated with a Seaglider to date. The forward fairing of the Seaglider was extended by 40 cm with a fiberglass cylindrical extension to create internal wet payload space for the sensor, pump, and cables (Figure 1 a and b). The sensor was mounted with the membrane facing aft to ensure that

https://doi.org/10.5194/egusphere-2024-1055
Preprint. Discussion started: 11 April 2024

potential bubbles within the internal tubing of the sensor could escape the system during the downcast of the first dive. In situ comparison of the orientation of the sensor suggested the highest data quality is achieved with this mounting design.

One of the advantages of using ocean gliders for ocean observing is the ability for real-time communication of data and commands between the pilot and the glider. To take advantage of this, modifications were needed to allow two-way communication between the Seaglider firmware and the HydroC firmware. The Seaglider firmware has a feature to allow easy integration of "logging devices," which provides a way to build commands for the pilot on land to switch the sensor on and off and change sampling strategy during the mission (on/off below or above certain depth) when it comes to the surface for a communication session. The Seaglider firmware can also automatically set the clock of the sensor on request at every surfacing and send small samples of the data stream via Iridium along with the standard sensor data. This required the writing and testing of a driver file (CNF file). However, to take full advantage of the ability of the HydroC, a more-advanced electronic integration was carried out using Smart Interoperable Real-time Maritime Assembly (SIRMA™, registered trademark of Cyprus Subsea Consulting and Services, C.S.C.S., Ltd.). This small programmable electronic circuit contains hardware elements to adapt the sensor power and communication requirements to those available on the host platform. It also allows for separate storage and processing capabilities to supplement the main host processor that controls the flight, sampling, and telecommunications of the host. Most importantly here, it was programmed to relay pilot commands to the SG HydroC CO_2 for the built-in "zero" function, which isolates the internal gas circuit until there is no CO_2 present, measures the concentration signal and assigns a zero value. Then the gas circuit is exposed to the head space behind the diffusion membrane for in situ sampling. SIRMA was also programmed to

https://doi.org/10.5194/egusphere-2024-1055
Preprint. Discussion started: 11 April 2024

extract raw data from the HydroC and calculate bin average of some of the output fields which are useful for real-time mission adaptation and confirmation of sensor operation. Three levels of output were allowed, depending on how much surfacing time could be tolerated before continuing the mission (Baud rate for Iridium is very low, on the order of 4800 bps).

In addition to the HydroC CO_2 sensor, the CO_2 Seaglider carried an Aanderaa 4831F optode, a compact optical oxygen sensor, which works on the principle of luminescence quenching by oxygen. The 4831F is equipped with a fast response sensing foil with a well characterized response time of 8 seconds. Aanderaa optodes measure absolute oxygen concentration and % saturation, are the most widely used on ocean gliders, and have been integrated into both Slocum and Seagliders (OceanGliders Oxygen SOP, 2024; Bittig et al., 2018). The OceanGliders community has developed a Standard Operating Procedure (SOP) that details everything from mounting, calibration, available sensors, piloting tips, response time correction, to post-processing (OceanGliders Oxygen SOP, 2024). The CO_2 Seaglider was also outfitted with an SBE CT sail and Wetlabs Ecopuck.

2.2 CH_4 Seaglider

We also integrated a modified version of the CONTROS HydroC CH_4 sensor (-4H-JENA engineering GmbH, Kiel, Germany) with the Seaglider. The SG HydroC CH_4 sensor has the same form factor as the SG HydroC CO_2 sensor, however, is 0.5 kg heavier with its Tunable Diode Laser Absorption Spectroscopy component, so the SG HydroC CH_4 must be integrated with changes to the glider's ballast.

2.3 Spring and winter CO_2 Seaglider missions

https://doi.org/10.5194/egusphere-2024-1055
Preprint. Discussion started: 11 April 2024

Both versions of the CO_2 Seaglider (rated to 300 m versus 1000 m) were tested in separate missions in spring and winter (Figure 3). The 300 m version with integrated POM housing was tested during a five-day long mission in May 2022. The glider followed along a transect within Resurrection Bay. CTD casts near the glider path allowed for in depth evaluation of the data quality. The 1000 m depth rated CO_2 Seaglider with integrated titanium housing was tested in February 2023.

2.4 Tank experiments

The glider was kept in a flow-through tank at the Alutiiq Pride Marine Institute for roughly 12h. The flow-through tank was fed with water from about 75 m depth and 91 m from the laboratory into Resurrection Bay, near a freshwater source. SG HydroC CO2T-0718-001 (Figure 4a, blue line) was integrated into the Seaglider. SG HydroC CO2T-0422-001 and the SG HydroC CH_4 sensors were installed on rocks next to the Seaglider. The water was kept in motion with a circulation pump. Triplicate discrete water samples for dissolved inorganic carbon, pH, and CH_4 analysis were taken every four hours.

2.5 Rosette package

The spare SG HydroC CO_2 sensor (CO2T-0422-001) was installed on an SBE-55 frame ECO water sampler with six 4-liter sample bottles (Seabird Scientific). The SBE-55 and SG HydroC CO_2 were controlled and powered by a SBE-33 carousel deck unit. The SG HydroC CO_2 interfered with the communication stream and thereby prevented real-time data acquisition and control of the SBE-55, however data were internally logged as required. Depth of the rosette

https://doi.org/10.5194/egusphere-2024-1055
Preprint. Discussion started: 11 April 2024

package was monitored directly on the winch and the timing of firing of the sample bottles during the upcast was programmed in advance based on time intervals.

2.6 Discrete water samples

2.6.1 Inorganic carbon chemistry

Discrete seawater samples were collected for sensor validation alongside two SG HydroC CO_2 sensors during a tank experiment at the Alutiiq Pride Marine Institute (Figure 4a, Table 1), from sample bottles mounted next to the SG HydroC CO_2 (Figure 1d), and from sample bottles during a CTD cast within 500 m and 30-60 minutes of the glider conducting dives (Section 3.2).

Inorganic carbon sampling in glaciated coastal regions requires methodological variations from open-ocean best practices to ensure that suspended mineral particles do not compromise the instrumentation and/or bias measurements between sample collection and analysis (Sejr et al., 2011). Given this, the discrete seawater samples were filtered (replaceable 0.45 µm filter in a 47 mm polycarbonate in-line filter) with a peristaltic pump straight from the Niskin bottles (see Bockmon and Dickson, (2014) for detailed method), or tank, into pre-cleaned 500 mL borosilicate bottles, and poisoned with 200 µL mercuric chloride ($HgCl_2$) (Dickson et al., 2007). Samples were transported and stored at room temperature before analysis. Samples were opened immediately (<5 minutes) before concurrent analyses of pH and DIC to limit gas exchange with ambient lab conditions.

Samples were analyzed for DIC using an Apollo SciTech, LLC Dissolved Inorganic Carbon Analyzer model AS-C6. All species of dissolved inorganic carbon in a sample are converted to CO_2 by the addition of a strong acid. The CO_2 gas is then purged from the sample through a drying system. The concentration of CO_2 gas is measured using a non-dispersive

https://doi.org/10.5194/egusphere-2024-1055
Preprint. Discussion started: 11 April 2024

infrared gas analyzer, the LI-7000 CO_2/H_2O Analyzer. This method requires Certified Reference Material (CRM) to create a three-point calibration line. The calibration line is used to quantify the total amount of CO_2 in the sample as the integrated area under the concentration-time curve. Apollo SciTech recommendations to improve analytical accuracy were followed and include bubbling of CO_2 off the acid daily, allowing the analyzer to warm up for at least 2 hours before measurements begin, measuring a set of standards at the beginning and end of each day and every 9 samples, using UHP (Ultra High Purity) N_2 gas, and filtering the N_2 gas with a PTFE filter, CO_2 scrubber (Ascarite II) and H_2O scrubber ($Mg(ClO_4)_2$).

Samples were analyzed spectrophotometrically for pH with a CONTROS HydroFIA pH (Aßmann et al., 2011) operating in discrete measurement mode using unpurified m-Cresol Purple (mCP) as the indicator dye (Clayton and Byrne, 1993). Sample temperature was stabilized at 25C+/-0.01 during measurements using Peltier elements and 5 repetitive measurements were taken for each sample. At the beginning of each day the HydroFIA pH underwent a conditioning period using seawater with similar properties until values stabilize. CRMs (known TA and DIC concentration) were measured at the beginning and end of the day, as well as every 9 samples.

All data manipulation and analyses were done using in-house MATLAB routine. In situ pH and pCO_2 were calculated from input pair pH_{lab} and DIC using CO2SYSv3 (Sharp et al., 2023) with dissociation constants for carbonic acid of Sulpis et al. (2020), bisulfate of (Dickson, 1990), hydrofluoric acid of Perez and Fraga, (1987), and the boron-to-chlorinity ratio of (Lee et al., 2010). Sulpis et al. (2020) found that the carbonic acid dissociation constants of Lueker et al. (2000) may underestimate pCO_2 in cold regions (below ~8°C) and, therefore, overestimate pH and CO_3^{-2}. Differences between discrete pCO_2 calculated with the carbonic acid dissociation constants by Lueker et al. (2000) (the standard in synthesis data products (e.g., Jiang et al., 2021,

https://doi.org/10.5194/egusphere-2024-1055
Preprint. Discussion started: 11 April 2024

Lauvset et al., 2022, Metzl et al., 2024) and the HydroC pCO_2 from the tank experiment were found to be on average 4.6 (1.6 %) and 4.2 (0.7 %) greater for SN0422 and SN0718, respectively, when compared with discrete pCO_2 based on carbonic acid dissociation constants by Sulpis et al. (2020).

Discrete pCO_2 uncertainty (u_c) is the combined standard uncertainty from *errors.m* (Orr et al., 2018) that propagates input uncertainties. Input uncertainties for pH_{lab} and DIC are the standard uncertainties, defined as the square root of the sum of the squared random uncertainty component plus the squared systematic uncertainty components. For pH_{lab} the random uncertainty is the sample precision, or standard deviation of the measurements. For DIC, the random uncertainty is the propagated error calculated with the first-order Taylor series expansion (Equation 1, Orr et al. (2018)) and assuming the correlation term is zero for the conversion of molarity (µmoles l^{-1}) to molality (µmoles kg^{-1}). Systematic uncertainty components are the uncertainty in the Certified Reference Material used for instrument offset and drift correction, and the published instrument accuracy, or if available, the daily instrument accuracy as defined below. Daily instrument accuracy is defined as the maximum difference between the known Certified Reference Material (CRM) concentration, and the measured CRM concentration after data were corrected for instrument drift and offset of all available CRM's not used in the instrument drift and offset calculation. CRM pH_{lab} "known" values are calculated using CO2SYSv3 (Sharp et al., 2023) with inputs pH and DIC. Nutrient concentrations (SiO_4^{-2}, PO_4^{-3}) were assumed to be negligible in the CO2SYS calculations (e.g. DeGrandpre et al. (2019); Vergara-Jara et al. (2019); Islam et al. (2017)).

2.6.2 Methane

https://doi.org/10.5194/egusphere-2024-1055
Preprint. Discussion started: 11 April 2024

Triplicate pCH_4 discrete water samples were collected every 4 hours during the tank experiment for an initial evaluation of the SG HydroC CH_4 sensor (Figure 4b). Seawater was filtered straight from the tank into 250 mL vials. The vials were closed with a rubber stopper, topped with an aluminum cap, and closed with a crimp immediately. A dry and clean syringe was flushed with 10 mL of N_2 gas twice. The third fill was kept, and the syringe valve was closed. N_2 was then injected into the headspace while simultaneously pulling 10 mL seawater out of the vial using a second syringe. 50 µL mercuric chloride ($HgCl_2$) were added to the vial, which was then shaken for about a minute and put into a fridge at 4°C for over 12 h to equilibrate the headspace. The samples were then sent to the Kessler analytical laboratory at the University of Rochester for analysis.

2.7 Data post-processing

2.7.1 pCO_2 post-processing

SG HydroC CO_2 data were post-processed using Jupyter notebook scripts developed by -4H-JENA Engineering GmbH at the original 2 second resolution. SG HydroC CO_2 data from the rosette mounted sensor (SG HydroC CO2T-0422-001) were post-processed using pre- and post-calibration coefficients interpolated with any change in the zero signal reference over the deployment (Fietzek et al., 2014). For the Seaglider integrated SG HydroC CO_2 sensor (SG HydroC CO2T-0718-001), data were post-processed with pre-calibration coefficients only because the sensor was damaged during the return shipment for post-calibration. Differences between sensors remained low despite the difference in processing, with a mean difference during the tank experiment of 2.12 ± 0.98 µatm (0.92%) and median difference of 2.00 ± 0.98

https://doi.org/10.5194/egusphere-2024-1055
Preprint. Discussion started: 11 April 2024

291 µatm (0.88%). The pCO_2 data from the February 2023 were not post-processed because a
292 required parameter was not relayed in real-time.

293 *2.7.2 Response time correction*

294 The ability to determine the in situ response time of the sensor enables the user to correct
295 for hysteresis through data post processing, critical for a sensor operating on profiling platforms
296 or anywhere where strong environmental gradients are encountered. Fiedler et al. (2013) used a
297 CONTROS HydroC™ CO_2 with a silicone, polydimethylsiloxane (PDMS) membrane and
298 reported a linear response time dependency on water temperature on the order of -1 s per 1 °C.
299 For this study, the SG HydroC CO_2 sensors were deployed with the new robust TOUGH
300 membrane, which uses Teflon AF2400 as the active separation layer and which has a low
301 temperature dependence on the permeability coefficient (Pinnau and Toy, 1996), so no
302 temperature dependency on our sensor's response times were observed. The response time with
303 the HydroC CO_2 TOUGH membrane is very stable but can be affected by the speed of water
304 exchange across the membrane (e.g. pump speed, tube length, etc.). Field verification of the
305 response time is recommended to ensure the highest quality post-processed data product. Our in
306 situ response time tests suggest to be within 5 seconds of the response time found during
307 calibration (not shown). The response time can be verified in the lab in a bucket or tank, or at
308 deployment or recovery when the glider is stationary for approximately 15 minutes and pCO_2
309 concentrations are stable by performing a zeroing interval with the HydroC CO_2 and reviewing
310 the time it takes for the signal to recover to the ambient concentration.
311 Response times were determined during calibration at -4H-JENA and found to be 106
312 and 108 seconds for HydroC CO2T-0422-001 when mounted on the rosette in May 2022 and

https://doi.org/10.5194/egusphere-2024-1055
Preprint. Discussion started: 11 April 2024

when integrated onto the Seaglider in February 2023, respectively. The response time of the sensor integrated into the Seaglider in May 2022 (HydroC CO2T-0718-001) was 109 seconds. A one-minute average was taken before response time correction was applied. Response time correction (RTC) was applied with 60 second resolution using the publicly available code from Dølven et al. (2022). There was no major difference (not shown) in RTC pCO_2 between the Dølven et al. (2022) and an RTC method (Miloshevich et al., 2004) previously used for HydroC CO_2 correction from a profiling float (Fielder et al. 2013), so we opted to use the Dølven et al. (2022) algorithm since it was developed with equilibrium-based sensors in mind and proven with a sensor with a long response time (HydroC CH_4 $\boldsymbol{\tau}_{63} \cong 23$ minutes).

2.7.3 pCH_4 post-processing

For the best possible accuracy, HydroC CH_4 sensors should be returned to -4H-JENA engineering GmbH for a post deployment performance verification. This includes a response time verification in the calibration tank at the pre-deployment verification conditions, as well as at the water temperature found in the field covering typical pCH_4 changes. A verification of the detector stability using reference gases with an accuracy of 0.5% can be provided. A response time of ~25 minutes was found with a 5T pump (Seabird Electronics) and found to be ~1.7 times slower with a 5M pump (Seabird Electronics). Response time correction was applied using a response time of ~43 minutes and the publicly available code from Dølven et al. (2022) (Figure 4b).

3. Results

3.1 Glider flight

https://doi.org/10.5194/egusphere-2024-1055
Preprint. Discussion started: 11 April 2024

Despite the large payload and major changes to the vehicle fairing, the glider was able to "fly" properly, allowing the desired undisturbed flow to meet the sensor's requirements. Example flight profiles from the 300 m and 1000 m configurations are shown in Figures 5 and 6. Pitch and vertical velocity are in the stable range, and roughly symmetric between downcast and upcast, indicating a nearly balanced glider. Heading varies around the targeted value as the roll adjusted to heading errors. It should be noted that this level of variability is typical of standard Seagliders. Operating Seagliders in shallow water (<200 m) is risky because of the likelihood of meeting depth-averaged currents of the same order of magnitude as the vehicle speed. A typical single dive cycle of downcast and upcast shows that the sensor data are free of noise that could be expected if there were recirculated water from the glider meeting the sensors. The expected endurance of the CO_2 Seaglider is around 18 days and 15 days for the CH_4 Seaglider with constant sampling at full depth.

3.2 CO_2 Seaglider data evaluation

The quality of the CO_2 Seaglider data was thoroughly tested with discrete and underway measurements during a tank experiment and glider missions.

3.2.1 Tank experiment

Discrete water samples show good agreement with the CO_2 Seaglider data (Figure 4a, Table 1). The values of discrete water samples represent the average of triplicate samples (Figure 4a, red dots). Differences between the HydroC CO_2 sensors remained low, with a mean difference during the tank experiment of 2.12 ± 0.98 µatm (0.91%) and median difference of

https://doi.org/10.5194/egusphere-2024-1055
Preprint. Discussion started: 11 April 2024

2.00 µatm (0.88%, Table 1). Percent differences (Eq. 1) between the HydroC CO_2 sensors and discrete water samples collected in the tank were between 0.2 and 1.7 % (Table 1, Figure 4).

$$\%\ difference\ = \frac{|{pCO_2}^{HydroC} - {pCO_2}^{disc}|}{({pCO_2}^{HydroC} + {pCO_2}^{disc})} * 100\% \qquad \text{(Equation 1)}$$

3.2.2 Profiling experiment

Rosette-based profiles with the SG HydroC CO_2 sensor in combination with discrete water samples were used to test and evaluate the response correction algorithm by Dølven et al. (2022). The rosette was lowered into the water and kept at 5m, 20m, 40m, 60m and 80m for about 20 minutes at a time (Figure 7a). Sample bottles were programmed to collect seawater toward the end of each hovering period. pCO_2 ranged from 219 µatm at the surface to 409 µatm at 80 m depth (Figure 7b). Differences between the SG HydroC CO_2 sensor and discrete samples ranged from -2.3 µatm (0.9 %) to 9.3 µatm (4.2%) (Table 2).

3.2.3 Data evaluation during CO_2 Seaglider mission

The quality of the pCO_2 data from the CO_2 Seaglider was further evaluated during a 3-day long sea trial mission in spring 2022 in Resurrection Bay, Alaska (Figure 3). Discrete water samples were taken in proximity (500 m) and within 30 - 60 minutes of the downcast of dive #51 (Figures 8 and 9a, Table 3). The response time corrected CO_2 Seaglider data compares well with the discrete water samples (Figure 8, dashed black line), overestimating the discrete water samples between 6.6 µatm (2.1 %) and 15.1 µatm (6.3 %) (Table 3).

3.3 CH_4 Seaglider data evaluation

https://doi.org/10.5194/egusphere-2024-1055
Preprint. Discussion started: 11 April 2024

379 3.3.1 Tank experiment

380 The SG HydroC CH_4 was also evaluated during the tank experiment described in section
381 2.4 (Figure 4c). During the experiment there was a decrease in salinity from 30.95 to 29.88 and
382 pCO_2 correspondingly decreased by 83 µatm. The corresponding pCH_4 RTC signal decreased
383 from 31.8 µatm to 6.6 µatm. Although the triplicate discrete pCH_4 water samples were slightly
384 lower than the sensor measured pCH_4 values, they also reflected this step change.

385

386 **3.4 Winter and springtime pCO_2 in Resurrection Bay, Alaska**

387 The surface to subsurface pCO_2 gradient is much larger in spring than in winter (Figure
388 10). During the early May mission, average surface pCO_2 was 240.8 +/- 17.6 µatm (mean +/-
389 standard deviation at 1 meter) with an average temperature of 5.9 +/- 0.4 °C (Figures 9 and 10).
390 In February, surface pCO_2 was near atmospheric pCO_2 (420.5 +/- 11.3 µatm, temperature 4.0 +/-
391 0.3 °C) and about 180 µatm higher than in May (Figures 10 and 11). As a comparison, NOAA's
392 moored sensor located in Sunny Cove (59.911 °N, -149.35 °W), near the CO_2 Seaglider trial site,
393 measured an average surface pCO_2 of 240.7 +/- 10.4 µatm during the time of the May 2022
394 mission and a minimum of 140 µatm in mid-April (3-day average) (Figure 12, Monacci et al.,
395 2023), suggesting that the peak of the spring bloom happened three weeks prior to our glider
396 mission. Since we don't have salinity data from the May CO_2 glider mission (conductivity sensor
397 failure), we cannot disentangle the contributions of freshwater or primary production on the low
398 surface pCO_2 values that were observed during the May mission (Figure 9). The moored sensor
399 in Sunny Cove measured an average surface pCO_2 of 416.4 +/- 4.2 µatm during the time of the
400 February mission, straddling the atmospheric pCO_2 values (Monacci et al., 2023, Figure 12).
401 Subsurface pCO_2 at 180 m was on average 546.8 +/- 16.0 µatm during the February mission and

https://doi.org/10.5194/egusphere-2024-1055
Preprint. Discussion started: 11 April 2024

516.3 +/- 32.7 µatm during the May mission (Figure 10a). pCO_2 was much lower in May than in February throughout the upper water column (<120 m), whereas there was not much of a seasonal difference at deeper depth. Some of the fine scale features apparent in the May pCO_2 and O_2 profiles are likely due to various levels of photosynthetic activity (Figure 10). As the glider transitioned into the open Gulf of Alaska during the February mission, water with O_2 < 150 µM shoaled into the upper 150 m of the water column (Figure 11). Unfortunately, the HydroC CO_2 sensor was turned off at that stage of the mission to conserve battery.

4. Discussion

The newly developed CO_2 Seaglider is the first of its kind to autonomously collect high quality pCO_2 data down to 1000 m depth. The tank and rosette experiments and in situ data evaluation suggest that the post-processed data from the CO_2 Seaglider generally fall near the relative uncertainty of 2.5%, which is a threshold defined as the "quality sufficient to identify relative spatial patterns and short-term variation" ("weather quality", Newton et al., 2015). This is the highest quality of pCO_2 data that has been measured with a subsurface autonomous vehicle to this date and therefore an important step towards filling the subsurface pCO_2 data gap in glider accessible regions.

The newly developed CO_2 Seaglider is suitable for data collection in open ocean or coastal environments with bottom depths deeper than 300 m. However, the coastal Gulf of Alaska is a highly dynamic environment, with strong freshwater and wind influence, and rugged shallow (often < 200 m) bottom topography. Strong currents (up to 0.50 m s^{-1}) made the piloting of the glider extremely difficult throughout the project and confirmed that the Seaglider cannot reliably reach desired waypoints in these conditions. The current version of the CO_2 Seaglider is

https://doi.org/10.5194/egusphere-2024-1055
Preprint. Discussion started: 11 April 2024

also not suitable for operating in the coastal Gulf of Alaska in summer and early fall, due to strong seasonal salinity gradients in this freshwater influenced area. Another issue we faced was the fact that the transducer did not work in its position behind the HydroC CO_2. In areas with detailed topography maps this would not be an issue, but in the coastal Gulf of Alaska reliable topography information is not readily available yet. An obvious next step is to integrate the SG HydroC CO_2 sensor into a newer glider platform, such as the Seaglider SGX or Teledyne Slocum G3 glider. The extended energy bay, larger buoyancy range, and thruster should make the operation of the coastal Slocum G3 with HydroC sensors relatively easy and would allow for autonomous high-resolution water column measurements of pCO_2 and pCH_4 in dynamic coastal environments. The integration of a HydroC on a Slocum glider will require a custom-made wet-payload bay due to the size of this sensor. For open ocean or deeper coastal regions, the integration with the Seaglider SGX, with 60% higher energy capacity, would be effective and nearly identical to the work already done here.

The SG HydroC CH_4 was successfully integrated into the Seaglider as part of this project. While the results from our initial tank experiments look promising, the CH_4 Seaglider still needs to be thoroughly tested in an environment with strong pCH_4 gradients to fully evaluate the glider-based pCH_4 response time corrected data. -4-H JENA is currently developing a combined HydroC CH_4/CO_2 sensor with the same form factor as the current HydroC CO_2 and CH_4 sensors, which will make integration into the Seaglider or other platforms relatively simple and open new opportunities to monitor both gases at the same time.

Ocean gliders are part of the Intergovernmental Oceanographic Commission (IOC-UNESCO) Global Ocean Observing System (GOOS) through the OceanGliders program (https://www.oceangliders.org/). Like other elements of the GOOS coordinated by OceanOPs of

https://doi.org/10.5194/egusphere-2024-1055
Preprint. Discussion started: 11 April 2024

the Observation Coordination Group (floats, buoys, moorings, ships, and tide gauges), OceanGliders contributes to "Ocean Observation for Climate, Ocean Health and Real Time Services". CO_2 and CH_4 gliders are perfectly suited to contribute data related to the respective global cycles of those compounds, for understanding relevant processes in coastal shelf and boundary regions where mesoscale or sub-mesoscales dominate. The current work can also serve as a first step to bring together interested scientists and engineers to further develop and improve the capability of gliders to measure high quality data. OceanGliders supports this effort through promoting formation of volunteer international task teams, for which a task team could be requested for oceanographic greenhouse gas research. By doing this, the visibility and availability of data will be improved as well, since GOOS provides an interactive data platform for all its programs (https://www.ocean-ops.org/board). An OceanGliders task team could also be linked with the GOOS-sponsored Global Climate Observing System (GCOS: https://gcos.wmo.int/en/home) program through their Ocean Observations Physics and Climate Panel (OOPC): "a scientific expert advisory group charged with making recommendations for a sustained global ocean observing system for climate."

5. Concluding Thoughts

Near real time and high-resolution water column data that can be retrieved from gliders outfitted with sensors measuring salinity, temperature, inorganic carbon system parameters, oxygen, and pCH_4 are key to tackle a variety of today's climate change related issues. These datasets will become instrumental to advance biogeochemical model forecasting and early warning systems for extreme heat, acidity and oxygen compound events that affect coastal subsistence communities, commercial fisheries, and mariculture. Furthermore, using

https://doi.org/10.5194/egusphere-2024-1055
Preprint. Discussion started: 11 April 2024

biogeochemical gliders to monitor the environment of tagged organisms (e.g. crabs, fish) would provide insight into the organism's position and behavior relative to important environmental drivers across susceptible ecosystems. Such biogeochemical glider data will help bridge in situ chemical and biological measurements, and environmental change to impacts on biology, and thereby fill an important research gap (Widdicomb et al., 2023). Potentially large natural and anthropogenic sources of CH_4 may become contributors to climate change, and if oxidized, to ocean acidification (Garcia-Tigreros et al., 2021; Sparrow et al., 2018; Shakhova et al., 2010; Rees et al., 2022). These CH_4 sources need to be properly assessed, quantified, and if characterized of anthropogenic origin, emitters must be held accountable (Goodman et al., 2022). Once the combined HydroC CH_4/CO_2 is available it will provide a new tool to co-measure pCH_4 and pCO_2 and give valuable insight into these processes and feedback mechanisms. Other advancing fields, such marine Carbon Dioxide Removal (mCDR) and monitoring, verification, and reporting (MRV) thereof will also need detailed knowledge of the distribution of CO_2 in the water column (National Academies of Sciences, Engineering, and Medicine. 2022).

The CO_2 Seaglider has been extensively tested and is ready to be used in open ocean environments. An important next step will be to integrate the HydroC CO_2 and CH_4 sensors into a glider platform that reliably functions in shallow, and freshwater affected coastal areas, such as the Gulf of Alaska, to be able to fill the large spatial and temporal data gap in these highly dynamic areas.

Data availability

The data is currently being prepared for publication on Pangaea.de.

https://doi.org/10.5194/egusphere-2024-1055
Preprint. Discussion started: 11 April 2024

Author contributions

C.H. and A.M. developed the research ideas and the proposal that funded this work. C.H. led the fieldwork and writing of this manuscript. B.I. led the preparation for fieldwork and glider data analysis. D.H. led glider piloting for all trials. D.H. and E.A. assisted with data processing, sensor programming, mechanical integration, glider ballasting, deployment, and recovery. N.K. and J.K. provided technical support for the HydroC sensors. All authors contributed to the writing of this manuscript.

Competing interests

The authors have no competing interests.

Acknowledgments

The Seaglider field trials took place in the traditional and contemporary hunting grounds of the Sugpiaq People. We also acknowledge that our Fairbanks-based offices are located on the Native lands of the Lower Tanana Dena. The Indigenous Peoples never surrendered lands or resources to Russia or the United States. We acknowledge this not only because we are grateful to the Indigenous communities who have been in deep connection with the land and water for time immemorial, but also in recognition of the historical and ongoing legacy of colonialism. We are committed to improving our scientific approaches and working towards co-production for a better future for everyone.

We would like to thank Jack Triest for his technical support throughout the project. We are also grateful to Brian Mullaly, Captain of the RV Nanuq, and Seward Marine Center staff, especially Pete Shipton, Ed DeCastro, Jenny Grischuk, and Jenny Elhard for their assistance

https://doi.org/10.5194/egusphere-2024-1055
Preprint. Discussion started: 11 April 2024

517 during the field trials in Seward. We are also grateful for the support from the Alutiiq Pride
518 Marine Institute, Alaska Sealife Center, and the Autonomous Remote Technology Lab. Finally,
519 we would like to express our gratitude to John Kessler and Katherine Gregory for analyzing our
520 CH_4 discrete water samples, guiding us through the sampling process and discussing CH_4
521 Seaglider missions with us. We would also like to thank for the support of Cyprus Subsea
522 engineers Sergey Vekli, Loizos Groutas, and Jerald Reodica in mechanical and electronic sensor
523 integration and piloting, as well as assisting with Cyprus sea testing of the HydroC sensors and
524 CO_2 Seaglider.
525
526 **Financial support**
527 We would like to thank the National Oceanographic Partnership Program and the
528 National Science Foundation for the support of this project (OCE-1841948).

https://doi.org/10.5194/egusphere-2024-1055
Preprint. Discussion started: 11 April 2024

References

Aßmann, S., Frank, C., and Körtzinger, A.: Spectrophotometric high-precision seawater pH determination for use in underway measuring systems, Ocean Sci., 7, 597–607, https://doi.org/10.5194/os-7-597-2011, 2011.

Bittig, H. C., Körtzinger, A., Neill, C., van Ooijen, E., Plant, J. N., Hahn, J., Johnson, K. S., Yang, B., and Emerson, S. R.: Oxygen Optode Sensors: Principle, Characterization, Calibration, and Application in the Ocean, Front. Mar. Sci., 4, https://doi.org/10.3389/fmars.2017.00429, 2018.

Bockmon, E. E. and Dickson, A. G.: A seawater filtration method suitable for total dissolved inorganic carbon and pH analyses, Limnology and Oceanography Methods, 12(4), 191–195, https://doi.org/10.4319/lom.2014.12.191, 2014.

Breitberg, D., Salisbury, J., Bernhard, J., Cai, W.-J., Dupont, S., Doney, S., Kroeker, K., Levin, L., Long, W. C., Milke, L., Miller, S., Phelan, B., Passow, U., Seibel, B., Todgham, A., and Tarrant, A.: And on Top of All That… Coping with Ocean Acidification in the Midst of Many Stressors, Oceanography, 25, 48–61, https://doi.org/10.5670/oceanog.2015.31, 2015.

Breitburg, D., Levin, L. A., Oschlies, A., Grégoire, M., Chavez, F. P., Conley, D. J., Garçon, V., Gilbert, D., Gutiérrez, D., Isensee, K., Jacinto, G. S., Limburg, K. E., Montes, I., Naqvi, S. W. A., Pitcher, G. C., Rabalais, N. N., Roman, M. R., Rose, K. A., Seibel, B. A., Telszewski, M., Yasuhara, M., and Zhang, J.: Declining oxygen in the global ocean and coastal waters, Science,

https://doi.org/10.5194/egusphere-2024-1055
Preprint. Discussion started: 11 April 2024

359, 46, https://doi.org/10.1126/science.aam7240, 2018.

Briggs, E. M., Martz, T. R., Talley, L. D., Mazloff, M. R., and Johnson, K. S.: Physical and Biological Drivers of Biogeochemical Tracers Within the Seasonal Sea Ice Zone of the Southern Ocean From Profiling Floats, J. Geophys. Res. Oceans, 123, 746–758, https://doi.org/10.1002/2017JC012846, 2018.

Chavez, F. P., Sevadjian, J., Wahl, C., Friederich, J., and Friederich, G. E.: Measurements of pCO_2 and pH from an autonomous surface vehicle in a coastal upwelling system, Deep Sea Res. Part II Top. Stud. Oceanogr., 151, 137–146, https://doi.org/10.1016/j.dsr2.2017.01.001, 2018.

Claustre, H., Johnson, K. S., and Takeshita, Y.: Observing the Global Ocean with Biogeochemical-Argo, Annu. Rev. Mar. Sci., 12, 23–48, https://doi.org/10.1146/annurev-marine-010419-010956, 2020.

Clayton, T. D. and Byrne, R. H.: Spectrophotometric seawater pH measurements: total hydrogen ion concentration scale calibration of m-cresol purple and at-sea results, Deep Sea Res. Part Oceanogr. Res. Pap., 40(10), 2115–2129, 1993.

DeGrandpre, M. D., Lai, C. Z., Timmermans, M. L., Krishfield, R. A., Proshutinsky, A., and Torres, D.: Inorganic Carbon and pCO_2 Variability During Ice Formation in the Beaufort Gyre of the Canada Basin, J. Geophys. Res. Oceans, 124, 4017–4028, https://doi.org/10.1029/2019JC015109, 2019.

https://doi.org/10.5194/egusphere-2024-1055
Preprint. Discussion started: 11 April 2024

575

576 Dickson, A. G.: Thermodynamics of the dissociation of boric acid in synthetic seawater from
577 273.15 to 318.15 K, Deep Sea Res. Part Oceanogr. Res. Pap., 37, 755–766,
578 https://doi.org/10.1016/0198-0149(90)90004-F, 1990.

579

580 Dickson, A. G. G., Sabine, C. L., Christian J.R., Christian, J. R., and Christian J.R.: Guide to
581 Best Practices for Ocean CO_2 Measurements, PICES Spec. Publ. 3, 191, 2007.

582

583 Dølven, K. O., Vierinen, J., Grilli, R., Triest, J., and Ferré, B.: Response time correction of slow-
584 response sensor data by deconvolution of the growth-law equation, Geosci. Instrum. Methods
585 Data Syst., 11, 293–306, https://doi.org/10.5194/gi-11-293-2022, 2022.

586

587 Doney, S. C., Fabry, V. J., Feely, R. A., and Kleypas, J. A.: Ocean Acidification: The Other CO_2
588 Problem, Annu. Rev. Mar. Sci., 1, 169–192,
589 https://doi.org/10.1146/annurev.marine.010908.163834, 2009.

590

591 Fiedler, B., Fietzek, P., Vieira, N., Silva, P., Bittig, H. C., and Körtzinger, A.: In situ CO_2 and O_2
592 measurements on a profiling float, J. Atmospheric Ocean. Technol., 30, 112–126,
593 https://doi.org/10.1175/JTECH-D-12-00043.1, 2013.

594

595 Fietzek, P., Fiedler, B., Steinhoff, T., and Körtzinger, A.: In situ quality assessment of a novel
596 underwater pCO_2 sensor based on membrane equilibration and NDIR spectrometry, J.
597 Atmospheric Ocean. Technol., 31, 181–196, https://doi.org/10.1175/JTECH-D-13-00083.1,

https://doi.org/10.5194/egusphere-2024-1055
Preprint. Discussion started: 11 April 2024

2014.

Garcia-Tigreros, F., Leonte, M., Ruppel, C. D., Ruiz-Angulo, A., Joung, D. J., Young, B., and Kessler, J. D.: Estimating the Impact of Seep Methane Oxidation on Ocean pH and Dissolved Inorganic Radiocarbon Along the U.S. Mid-Atlantic Bight, J. Geophys. Res. Biogeosciences, 126, e2019JG005621, https://doi.org/10.1029/2019JG005621, 2021.

Goodman, S., Davies, P., Maddox, M., and Durkee, J.: Arctic Methane – Situational Awareness, Assessment and Policy Directions, Results of the June 23rd, 2022 Arctic Methane Workshop, Summary Report, 2022.

Gruber, N., Clement, D., Carter, B. R., Feely, R. A., van Heuven, S., Hoppema, M., Ishii, M., Key, R. M., Kozyr, A., Lauvset, S. K., Lo Monaco, C., Mathis, J. T., Murata, A., Olsen, A., Perez, F. F., Sabine, C. L., Tanhua, T., and Wanninkhof, R.: The oceanic sink for anthropogenic CO2 from 1994 to 2007, Science, 363, 1193–1199, https://doi.org/10.1126/science.aau5153, 2019.

Gruber, N., Boyd, P. W., Frölicher, T. L., and Vogt, M.: Biogeochemical extremes and compound events in the ocean, Nature, 600, 395–407, https://doi.org/10.1038/s41586-021-03981-7, 2021.

Hauri, C., McDonnell, A., Winsor, P., Irving, B., and Statscewich, H.: Development of an Autonomous Carbon Glider to Monitor Sea-Air CO_2 Fluxes in the Chukchi Sea, Bureau of

https://doi.org/10.5194/egusphere-2024-1055
Preprint. Discussion started: 11 April 2024

Ocean Energy Management, 2018.

Hauri, C., Pagès, R., Hedstrom, K., Doney, S. C., Dupont, S., Ferriss, B., and Stuecker, M. F.: More Than Marine Heatwaves: A New Regime of Heat, Acidity, and Low Oxygen Compound Extreme Events in the Gulf of Alaska, AGU Adv., 5, e2023AV001039, https://doi.org/10.1029/2023AV001039, 2024.

Hemming, M. P., Kaiser, J., Heywood, K. J., Bakker, D. C. E., Boutin, J., Shitashima, K., Lee, G., Legge, O., and Onken, R.: Measuring pH variability using an experimental sensor on an underwater glider, Ocean Sci., 13, 427–442, https://doi.org/10.5194/os-13-427-2017, 2017.

Islam, F., DeGrandpre, M. D., Beatty, C. M., Timmermans, M.-L., Krishfield, R. A., Toole, J. M., and Laney, S. R.: Sea surface CO_2 and O_2 dynamics in the partially ice-covered Arctic Ocean, J. Geophys. Res. Oceans, 122, 1425–1438, https://doi.org/10.1002/2016JC012162, 2017.

Jiang, L.-Q., Feely, R. A., Wanninkhof, R., Greeley, D., Barbero, L., Alin, S., Carter, B. R., Pierrot, D., Featherstone, C., Hooper, J., Melrose, C., Monacci, N., Sharp, J. D., Shellito, S., Xu, Y.-Y., Kozyr, A., Byrne, R. H., Cai, W.-J., Cross, J., Johnson, G. C., Hales, B., Langdon, C., Mathis, J., Salisbury, J., and Townsend, D. W.: Coastal Ocean Data Analysis Product in North America (CODAP-NA) – an internally consistent data product for discrete inorganic carbon, oxygen, and nutrients on the North American ocean margins, Earth Syst. Sci. Data, 13, 2777–2799, https://doi.org/10.5194/essd-13-2777-2021, 2021.

https://doi.org/10.5194/egusphere-2024-1055
Preprint. Discussion started: 11 April 2024

644 Johnson, G. C. and Lyman, J. M.: Warming trends increasingly dominate global ocean, Nat.
645 Clim. Change, 10, 757–761, https://doi.org/10.1038/s41558-020-0822-0, 2020.
646
647 Kroeker, K. J., Kordas, R. L., and Harley, C. D. G.: Embracing interactions in ocean
648 acidification research: Confronting multiple stressor scenarios and context dependence, Biol.
649 Lett., 13, https://doi.org/10.1098/rsbl.2016.0802, 2017.
650
651 Laufkötter, C., Zscheischler, J., and Frölicher, T. L.: High-impact marine heatwaves attributable
652 to human-induced global warming, Science, 369, 1621–1625,
653 https://doi.org/10.1126/science.aba0690, 2020.
654
655 Lauvset, S. K., Lange, N., Tanhua, T., Bittig, H. C., Olsen, A., Kozyr, A., Alin, S., Álvarez, M.,
656 Azetsu-Scott, K., Barbero, L., Becker, S., Brown, P. J., Carter, B. R., da Cunha, L. C., Feely, R.
657 A., Hoppema, M., Humphreys, M. P., Ishii, M., Jeansson, E., Jiang, L.-Q., Jones, S. D., Lo
658 Monaco, C., Murata, A., Müller, J. D., Pérez, F. F., Pfeil, B., Schirnick, C., Steinfeldt, R.,
659 Suzuki, T., Tilbrook, B., Ulfsbo, A., Velo, A., Woosley, R. J., and Key, R. M.:
660 GLODAPv2.2022: the latest version of the global interior ocean biogeochemical data product,
661 Earth Syst. Sci. Data, 14, 5543–5572, https://doi.org/10.5194/essd-14-5543-2022, 2022.
662
663 Lee, K., Kim, T.-W., Byrne, R. H., Millero, F. J., Feely, R. A., and Liu, Y.-M.: The universal
664 ratio of boron to chlorinity for the North Pacific and North Atlantic oceans, Geochim.
665 Cosmochim. Acta, 74, 1801–1811, https://doi.org/10.1016/j.gca.2009.12.027, 2010.
666

https://doi.org/10.5194/egusphere-2024-1055
Preprint. Discussion started: 11 April 2024

667 Lueker, T. J., Dickson, A. G., and Keeling, C. D.: Ocean pCO_2 calculated from dissolved
668 inorganic carbon , alkalinity , and equations for K 1 and K 2 : validation based on laboratory
669 measurements of CO_2 in gas and seawater at equilibrium, Mar. Chem., 70, 105–119,
670 https://doi.org/10.1016/S0304-4203(00)00022-0, 2000.
671
672 Manley, J. and Willcox, S.: The Wave Glider: A persistent platform for ocean science, in:
673 OCEANS'10 IEEE SYDNEY, OCEANS'10 IEEE SYDNEY, 1–5,
674 https://doi.org/10.1109/OCEANSSYD.2010.5603614, 2010.
675
676 Metzl, N., Fin, J., Lo Monaco, C., Mignon, C., Alliouane, S., Antoine, D., Bourdin, G., Boutin,
677 J., Bozec, Y., Conan, P., Coppola, L., Diaz, F., Douville, E., Durrieu de Madron, X., Gattuso, J.-
678 P., Gazeau, F., Golbol, M., Lansard, B., Lefèvre, D., Lefèvre, N., Lombard, F., Louanchi, F.,
679 Merlivat, L., Olivier, L., Petrenko, A., Petton, S., Pujo-Pay, M., Rabouille, C., Reverdin, G.,
680 Ridame, C., Tribollet, A., Vellucci, V., Wagener, T., and Wimart-Rousseau, C.: A synthesis of
681 ocean total alkalinity and dissolved inorganic carbon measurements from 1993 to 2022: the
682 SNAPO-CO2-v1 dataset, Earth Syst. Sci. Data, 16, 89–120, https://doi.org/10.5194/essd-16-89-
683 2024, 2024.
684
685 Meurer, W. P., Blum, J., and Shipman, G.: Volumetric Mapping of Methane Concentrations at
686 the Bush Hill Hydrocarbon Seep, Gulf of Mexico, Front. Earth Sci., 9,
687 https://doi.org/10.3389/feart.2021.604930, 2021.
688
689 Monacci, N.M.; Bott, R.; Cross, J.N.; Dougherty, S.; Maenner, S.; Musielewicz, S.; Osborne, J.;

https://doi.org/10.5194/egusphere-2024-1055
Preprint. Discussion started: 11 April 2024

690 Sutton, A. (2023). High-resolution ocean and atmosphere pCO_2 time-series measurements from
691 mooring GAKOA_149W_60N. High-resolution ocean and atmosphere pCO_2 time-series
692 measurements from mooring GAKOA_149W_60N in the Gulf of Alaska (NCEI Accession
693 0116714). NOAA National Centers for Environmental Information. Dataset.
694 https://doi.org/10.3334/cdiac/otg.tsm_gakoa_149w_60n
695
696 Manley, J. and Willcox, S.: The Wave Glider: A persistent platform for ocean science, in:
697 OCEANS'10 IEEE SYDNEY, OCEANS'10 IEEE SYDNEY, 1–5,
698 https://doi.org/10.1109/OCEANSSYD.2010.5603614, 2010.
699
700 Miloshevich, L. M., Paukkunen, A., Vömel, H., and Oltmans, S. J.: Development and Validation
701 of a Time-Lag Correction for Vaisala Radiosonde Humidity Measurements, J. Atmospheric
702 Ocean. Technol., 21, 1305–1327, https://doi.org/10.1175/1520-
703 0426(2004)021<1305:DAVOAT>2.0.CO;2, 2004.
704
705 National Academies of Sciences, Engineering, and Medicine: A Research Strategy
706 for Ocean-based Carbon Dioxide Removal and Sequestration. Washington, DC: The National
707 Academies Press. https://doi.org/10.17226/26278, 2022.
708
709 Newton, J. A., Feely, R. A., Jewett, E. B., Williamson, P., and Mathis, J.: Global ocean
710 acidification observing network: requirements and governance plan, GOA-ON, Washington, 61
711 pp., 2015.
712

https://doi.org/10.5194/egusphere-2024-1055
Preprint. Discussion started: 11 April 2024

713 Nickford, S., Palter, J. B., Donohue, K., Fassbender, A. J., Gray, A. R., Long, J., Sutton, A. J.,
714 Bates, N. R., and Takeshita, Y.: Autonomous Wintertime Observations of Air-Sea Exchange in
715 the Gulf Stream Reveal a Perfect Storm for Ocean CO_2 Uptake, Geophys. Res. Lett., 49,
716 e2021GL096805, https://doi.org/10.1029/2021GL096805, 2022.
717
718 von Oppeln-Bronikowski, N., de Young, B., Atamanchuk, D., and Wallace, D.: Glider-based
719 observations of CO_2 in the Labrador Sea, Ocean Sci., 17, 1–16, https://doi.org/10.5194/os-17-1-
720 2021, 2021.
721
722 OceanGliders Oxygen SOP: https://nora.nerc.ac.uk/id/eprint/533559/, last access: 24 January
723 2024.
724
725 Orr, J. C., Epitalon, J. M., Dickson, A. G., and Gattuso, J. P.: Routine uncertainty propagation
726 for the marine carbon dioxide system, Mar. Chem., 207, 84–107,
727 https://doi.org/10.1016/j.marchem.2018.10.006, 2018.
728
729 Perez, F. F. and Fraga, F.: Association constant of fluoride and hydrogen ions in seawater, Mar.
730 Chem., 21, 161–168, https://doi.org/10.1016/0304-4203(87)90036-3, 1987.
731
732 Pinnau, I., and Toy, L. G.: Gas and vapor transport properties of amorphous perfluorinated
733 copolymer membranes based on 2,2-bistrifluoromethyl-4,5-difluoro-1,3-
734 dioxole/tetrafluoroethylene, Journal of Membrane Science, 109 (1), 125-133,
735 https://doi.org/10.1016/0376-7388(95)00193-X, 1996.

https://doi.org/10.5194/egusphere-2024-1055
Preprint. Discussion started: 11 April 2024

736

737 Possenti, L., Humphreys, M. P., Bakker, D. C. E., Cobas-García, M., Fernand, L., Lee, G. A.,
738 Pallottino, F., Loucaides, S., Mowlem, M. C., and Kaiser, J.: Air-Sea Gas Fluxes and
739 Remineralization From a Novel Combination of pH and O_2 Sensors on a Glider, Front. Mar. Sci.,
740 8, 1–19, https://doi.org/10.3389/fmars.2021.696772, 2021.

741

742 Qi, D., Ouyang, Z., Chen, L., Wu, Y., Lei, R., Chen, B., Feely, R. A., Anderson, L. G., Zhong,
743 W., Lin, H., Polukhin, A., Zhang, Y., Zhang, Y., Bi, H., Lin, X., Luo, Y., Zhuang, Y., He, J.,
744 Chen, J., and Cai, W. J.: Climate change drives rapid decadal acidification in the Arctic Ocean
745 from 1994 to 2020, Science, 377, 1544–1550, https://doi.org/10.1126/science.abo0383, 2022.

746

747 Rees, A. P., Bange, H. W., Arévalo-Martínez, D. L., Artioli, Y., Ashby, D. M., Brown, I.,
748 Campen, H. I., Clark, D. R., Kitidis, V., Lessin, G., Tarran, G. A., and Turley, C.: Nitrous oxide
749 and methane in a changing Arctic Ocean, Ambio, 51, 398–410, https://doi.org/10.1007/s13280-
750 021-01633-8, 2022.

751

752 Saba, G. K., Wright-Fairbanks, E., Chen, B., Cai, W. J., Barnard, A. H., Jones, C. P., Branham,
753 C. W., Wang, K., and Miles, T.: The Development and Validation of a Profiling Glider Deep
754 ISFET-Based pH Sensor for High Resolution Observations of Coastal and Ocean Acidification,
755 Front. Mar. Sci., 6, 1–17, https://doi.org/10.3389/fmars.2019.00664, 2019.

756

757 Sabine, C. L. and Tanhua, T.: Estimation of anthropogenic CO_2 inventories in the ocean., Annu.
758 Rev. Mar. Sci., 2, 175–98, https://doi.org/10.1146/annurev-marine-120308-080947, 2010.

https://doi.org/10.5194/egusphere-2024-1055
Preprint. Discussion started: 11 April 2024

Sabine, C. L., Feely, R. A., Gruber, N., Key, R. M., Lee, K., Bullister, J. L., Wanninkhof, R., Wong, C. S., Wallace, D. W. R., Tilbrook, B., Millero, F. J., Peng, T.-H., Kozyr, A., Ono, T., and Rios, A. F.: The oceanic sink for anthropogenic CO_2, Science, 305, 367–71, https://doi.org/10.1126/science.1097403, 2004.

Sejr, M. K., Krause-Jensen, D., Rysgaard, S., Sørensen, L. L., Christensen, P. B., and Glud, R. N.: Air-sea flux of CO_2 in arctic coastal waters influenced by glacial melt water and sea ice, Tellus B, 63, 815–822, https://doi.org/10.1111/j.1600-0889.2011.00540.x, 2011.

Sharp, J. D., Pierrot, D., Humphreys, M. P., Epitalon, J.-M., Orr, J. C., Lewis, E. R., and Wallace, D. W. R.: CO2SYSv3 for MATLAB, , https://doi.org/10.5281/zenodo.7552554, 2023.

Shakhova, N., Semiletov, I., Salyuk, A., Yusupov, V., Kosmach, D., and Gustafsson, Ö.: Extensive Methane Venting to the Atmosphere from Sediments of the East Siberian Arctic Shelf, Science, 327, 1246–1250, https://doi.org/10.1126/science.1182221, 2010.

Sparrow, K. J., Kessler, J. D., Southon, J. R., Garcia-Tigreros, F., Schreiner, K. M., Ruppel, C. D., Miller, J. B., Lehman, S. J., and Xu, X.: Limited contribution of ancient methane to surface waters of the U.S. Beaufort Sea shelf, Sci. Adv., 4, eaao4842, https://doi.org/10.1126/sciadv.aao4842, 2018.

https://doi.org/10.5194/egusphere-2024-1055
Preprint. Discussion started: 11 April 2024

781 Sulpis, O., Lauvset, S. K., and Hagens, M.: Current estimates of K and K appear inconsistent
782 with measured CO_2 system parameters in cold oceanic regions, Ocean Sci., 16, 847–
783 862, https://doi.org/10.5194/os-16-847-2020, 2020.
784
785 Takeshita, Y., Jones, B. D., Johnson, K. S., Chavez, F. P., Rudnick, D. L., Blum, M., Conner, K.,
786 Jensen, S., Long, J. S., Maughan, T., Mertz, K. L., Sherman, J. T., and Warren, J. K.: Accurate
787 pH and O_2 Measurements from Spray Underwater Gliders, J. Atmospheric Ocean. Technol., 38,
788 181–195, https://doi.org/10.1175/JTECH-D-20-0095.1, 2021.
789
790 Thompson, T., Saba, G. K., Wright-Fairbanks, E., Barnard, A. H., and Branham, C. W.: Best
791 Practices for Sea-Bird Scientific deep ISFET-based pH sensor integrated into a Slocum Webb
792 Glider, in: OCEANS 2021: San Diego – Porto, OCEANS 2021: San Diego – Porto, 1–8,
793 https://doi.org/10.23919/OCEANS44145.2021.9706067, 2021.
794
795 Vergara-Jara, M. J., DeGrandpre, M. D., Torres, R., Beatty, C. M., Cuevas, L. A., Alarcón, E.,
796 and Iriarte, J. L.: Seasonal changes in carbonate saturation state and air-sea CO_2 fluxes during an
797 annual cycle in a stratified-temperate fjord (Reloncaví Fjord, Chilean Patagonia), J. Geophys.
798 Res. Biogeosciences, 124, 2851–2865, https://doi.org/10.1029/2019jg005028, 2019.
799
800 Widdicombe, S., Isensee, K., Artioli, Y., Gaitán-Espitia, J. D., Hauri, C., Newton, J. A.,
801 et al.: Unifying biological field observations to detect and compare ocean acidification impacts
802 across marine species and ecosystems: What to monitor and why. *Ocean Science*, **19**(1), 101–
803 119. https://doi.org/10.5194/os-19-101-2023, 2023.

https://doi.org/10.5194/egusphere-2024-1055
Preprint. Discussion started: 11 April 2024

804

805 Woosley, R. J. and Millero, F. J.: Freshening of the western Arctic negates anthropogenic carbon

806 uptake potential, Limnol. Oceanogr., https://doi.org/10.1002/lno.11421, 2020.

807

808 Wright-Fairbanks, E. K., Miles, T. N., Cai, W.-J., Chen, B., and Saba, G. K.: Autonomous

809 Observation of Seasonal Carbonate Chemistry Dynamics in the Mid-Atlantic Bight, J. Geophys.

810 Res. Oceans, 125, e2020JC016505, https://doi.org/10.1029/2020JC016505, 2020.

811
812

813

814

815

https://doi.org/10.5194/egusphere-2024-1055
Preprint. Discussion started: 11 April 2024

816 **Tables**

817 **Table 1. Tank experiment.** Evaluation of SG HydroC CO_2 sensors compared to reference
818 discrete pCO_2 calculated with input pairs pH_{lab} and DIC. Units of pCO_2 are µatm except when
819 shown as percent difference in parenthesis (Equation 1). Columns with subscripts sn422 and
820 sn0718 indicate data from sensors HydroC CO2T-0422-001 and HydroC CO2T-0718-001,
821 respectively. Superscript RTC indicates response time corrected values following Dølven et al.
822 (2022). Values are the average of triplicate bottles and are shown in Figure 4.

Discrete Sample #	pCO_2^{disc} ± uc (µatm)	$pCO_{2,sn422}^{RTC}$ - pCO_2^{disc}	$pCO_{2,sn0718}^{RTC}$ - pCO_2^{disc}
1	298.7 ± 10.2	-1.1 (0.4%)	-
2	227.1 ± 7.8	3.9 (1.7%)	1.2 (0.5%)
3	223.3 ± 7.7	0.4 (0.2%)	-0.8 (0.4%)
4	227.8 ± 7.9	-0.6 (0.3%)	-3.1 (1.4%)

823

824

825 **Table 2. Profiling experiment.** Evaluation of SG HydroC CO_2 sensor compared to reference
826 discrete pCO_2^{disc} calculated with input pairs pH_{lab} and DIC. Units of pCO_2 are µatm except when
827 shown as percent difference in parenthesis (Eq. 1). pCO_2 with subscripts sn422 indicate data
828 from the HydroC installed on the rosette (HydroC CO2T-0422-001). The superscript RTC
829 indicates response time corrected values following Dølven et al. (2022). Asterisks (*) indicate

https://doi.org/10.5194/egusphere-2024-1055
Preprint. Discussion started: 11 April 2024

the comparison with rosette mounted SG HydroC CO_2 values taken as nearest in time before sensor zeroing.

Discrete Date Time (UTC)	Discrete Depth (m)	pCO_2^{disc} ± uc (µatm)	$pCO_{2,sn422}^{RTC}$ - pCO_2^{disc}
5/3/2022 21:21	2.5	214.5 ± 7.5	9.3 (4.2%)
5/3/2022 21:39	19.9	246.8 ± 8.5	3.4 (1.4%)
5/3/2022 22:33	9.6	244.4 ± 8.5	-2.3 (0.9%)
5/3/2022 22:34	9.7	234.7 ± 8.1	7.5 (3.2%)

Table 3. Seaglider HydroC evaluation with nearby cast. Evaluation of Seaglider integrated SG HydroC CO_2 sensor compared to discrete pCO_2^{disc} calculated with input pairs pH_{lab} and DIC collected from a rosette nearby. Units of pCO_2 are µatm except when shown as percent difference in parenthesis (Eq. 1). The superscript RTC indicates response time corrected values following Dølven et al. (2022). Distance columns represent the distance between when pCO_2 was measured on the Seaglider integrated HydroC to the time the discrete sample was collected and is given temporally (HH:MM) and spatially (km). $pCO_{2,sn422}^{RTC}$ is the rosette mounted SG HydroC CO2 sensor and $pCO_{2,sn0718}^{RTC}$ is the Seaglider mounted SG HydroC CO_2 sensor.

Discrete Date Time (UTC)	Discrete Depth (m)	pCO_2^{disc} ± uc (µatm)	Delay (HH:MM)	Distance (km)	$pCO_{2,sn0718}^{RTC}$ - pCO_2^{disc}
5/7/2022 18:06	72.5	349.7 ± 7.8	02:47	0.4	9.5 (2.7 %)
5/7/2022 18:24	57.7	313.8 ± 6.7	03:05	0.6	6.6 (2.1 %)
5/7/2022 18:42	20	285.3 ± 6.1	03:23	0.8	8.6 (3.0 %)
5/7/2022 19:00	1.6	233.4 ± 5.0	03:41	0.9	15.1 (6.3 %)

https://doi.org/10.5194/egusphere-2024-1055
Preprint. Discussion started: 11 April 2024

843 **Figures**

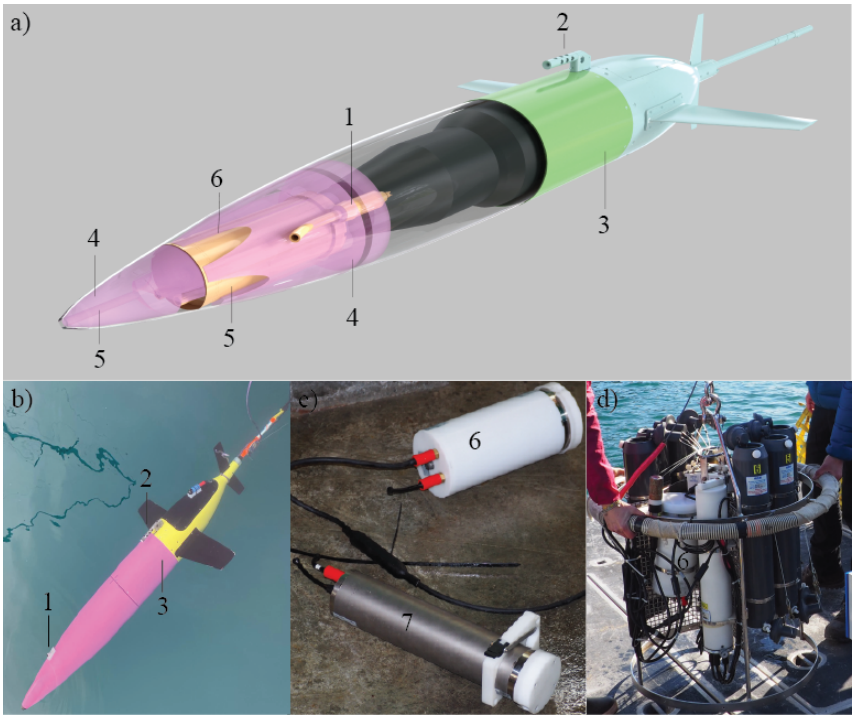

844

845 **Figure 1. CO_2 Seaglider.** CO_2 Seaglider a) schematic rendering and b) picture in Resurrection
846 Bay, Seward, Alaska, during a checkout dive on 6 February, 2023, before beginning the first
847 winter mission collecting high resolution pCO_2 data. Highlighted are 1) SeaBird 5M pump, 2)
848 conductivity and temperature sail, 3) extension, 4) syntactic foam, 5) water flow channels, and 6)
849 SG HydroC CO_2 in a titanium housing, enabling pCO_2 observations down to 1000 m. c) Picture
850 of new SG HydroC CO_2 in a POM housing (6, rated to 300 m depth) and original CONTROS
851 HydroC™ CO_2 (7). d) Picture of rosette set up for profiling experiment.

https://doi.org/10.5194/egusphere-2024-1055
Preprint. Discussion started: 11 April 2024

852

853 **Figure 2. SG HydroC CO_2 sensor mounting designs.** a) Titanium SG HydroC CO_2 (rated to

854 1000m) in a custom syntactic foam coat and b) POM SG HydroC CO_2 (rated to 300m) with

855 brackets.

https://doi.org/10.5194/egusphere-2024-1055
Preprint. Discussion started: 11 April 2024

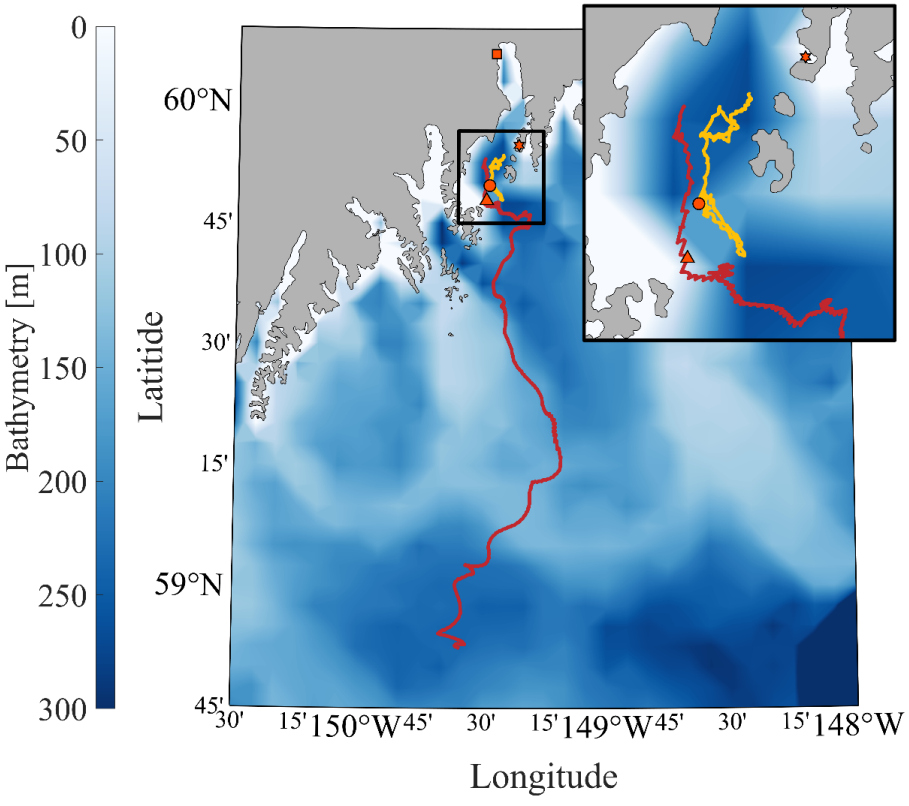

856

857 **Figure 3. Map of CO_2 Seaglider study area.** The bathymetry of the Gulf of Alaska is shown in
858 color with zoomed in section of the head of Resurrection Bay (outlined black square and inset
859 map). Tracks of the CO_2 Seaglider from the May 2022 and February 2023 missions are shown in
860 yellow and red, respectively. Orange markers outlined in black show the location of the Alutiiq
861 Pride Marine Institute (square), National Oceanic and Atmospheric Administration's Gulf of
862 Alaska Ocean Acidification mooring (star), May 7th CTD cast (circle), and last location where
863 pCO_2 was collected during the February 2023 mission (triangle).

864

https://doi.org/10.5194/egusphere-2024-1055
Preprint. Discussion started: 11 April 2024

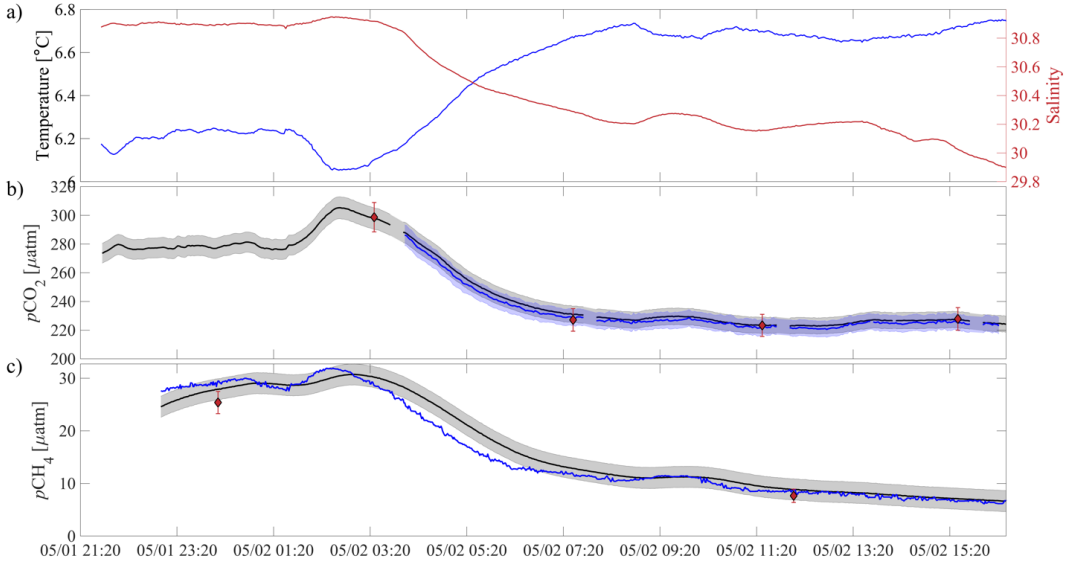

865

866 **Figure 4. Sensor validation during a tank experiment at the Alutiiq Pride Marine Institute**
867 **on May 1 – 2, 2022.** a) temperature (blue line) and salinity (red line) from a recently calibrated
868 Sea-Bird Scientific SBE37. b) black (blue) lines show pCO_2 in µatm from HydroC CO2T-0422-
869 001 (HydroC CO2T-0718-001) with the shaded gray (blue) areas showing a relative uncertainty
870 of 2.5% (weather quality goal; Newton et al., 2015). Black circles with red filling show discrete
871 pCO_2 calculated from input pair pH_{lab} and DIC with error bars showing the combined standard
872 uncertainty from *errors.m* (Orr et al., 2018). HydroC CO_2 data are shown at 1 minute resolution
873 with a 2-minute moving median filter applied and have not been corrected for response time, but
874 differences are negligible (Table 1). c) Black line shows pCH_4 in µatm from HydroC CH4T-
875 0422-001 with the shaded gray bar showing an uncertainty of 2 µatm (published instrument
876 accuracy of ± 2 µatm or ± 3%, whichever is greater). The blue line is the response time corrected
877 signal with a response time of 43 minutes following Dølven et al., (2022). HydroC CH_4 data are

https://doi.org/10.5194/egusphere-2024-1055
Preprint. Discussion started: 11 April 2024

878 shown at 1 minute resolution with a 2-minute moving median filter applied to the raw data and a
879 10-minute moving median filter applied to the RTC data. Black circles with red filling show
880 discrete pCH_4 and all discrete values of pCO_2 and pCH_4 are the average of triplicate bottles.
881

https://doi.org/10.5194/egusphere-2024-1055
Preprint. Discussion started: 11 April 2024

882

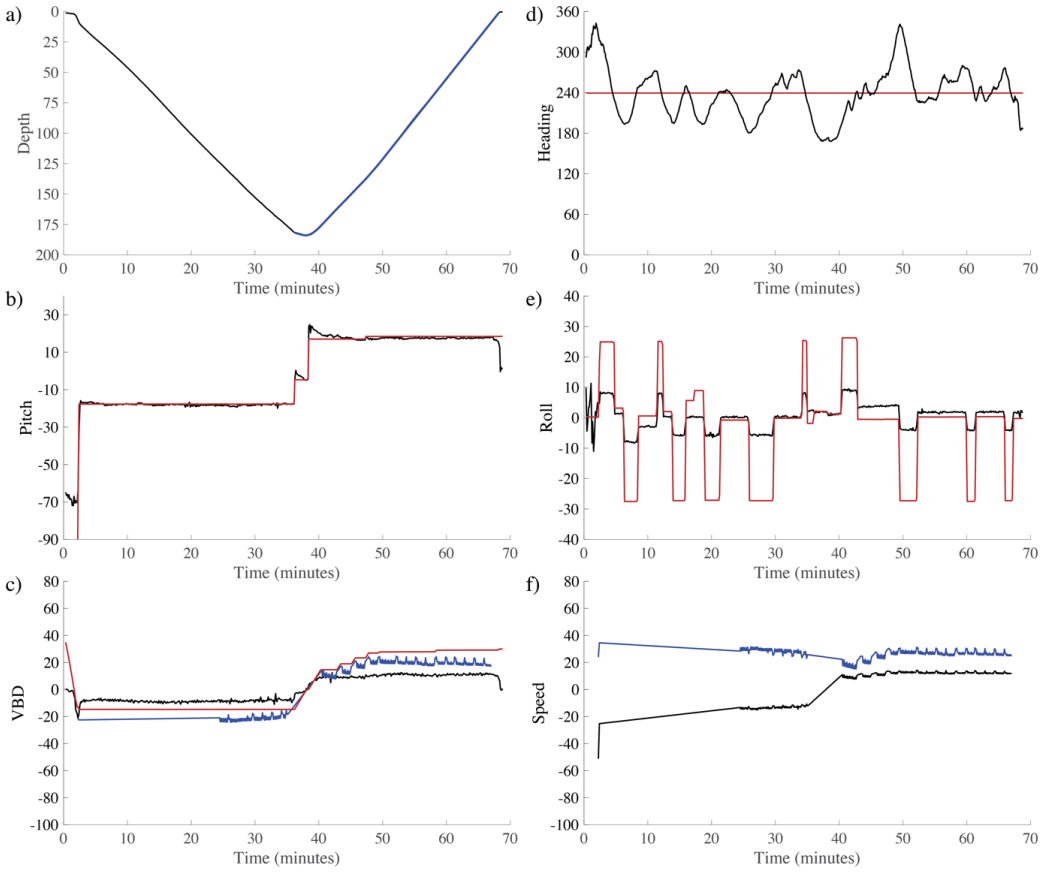

883

884 **Figure 5. Diveplot details for the 300 m rated CO_2 Seaglider (dive# 51).** a) Depth (black line,
885 meters), b) pitch (black line, degrees) with pitch control (red line, mm of battery shift), c)
886 Change in displacement of Variable Buoyancy Drive (VBD) (red line, units of 10 cc), vertical
887 velocity from pressure measurements (black line, cm/s), and buoyancy (blue line, units of 10 g),
888 d) heading in (desired red line, measured black line, degrees), e) roll (battery roll position red
889 line, glider measured roll black line, degrees), and f) vertical speed (calculated from buoyancy
890 and pitch, black line, cm/s) and horizontal speed (calculated from buoyancy and pitch, blue line,
891 cm/s).

https://doi.org/10.5194/egusphere-2024-1055
Preprint. Discussion started: 11 April 2024

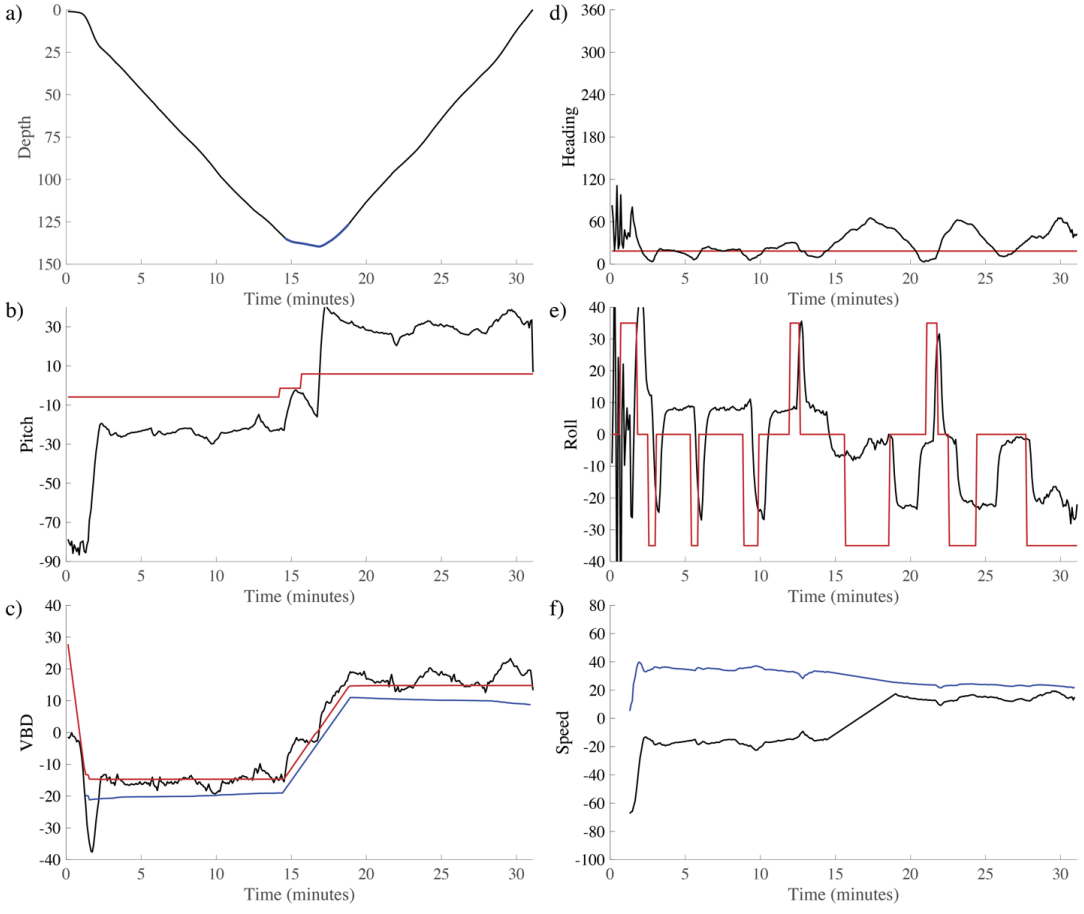

Figure 6. Diveplot details for the 1000 m rated CO_2 Seaglider (dive# 203). a) Depth (black line, meters), b) pitch (black line, degrees) with pitch control (red line, mm of battery shift), c) Change in displacement of Variable Buoyancy Drive (VBD) (red line, units of 10 cc), vertical velocity from pressure measurements (black line, cm/s), and buoyancy (blue line, units of 10 g), d) Heading (desired heading red line, measured heading black line, degrees) e) roll (battery roll position red line, glider measured roll black line, degrees), and f) vertical speed (calculated from buoyancy and pitch, black line, cm/s) and horizontal speed in cm/s (calculated from buoyancy and pitch, blue line, cm/s).

https://doi.org/10.5194/egusphere-2024-1055
Preprint. Discussion started: 11 April 2024

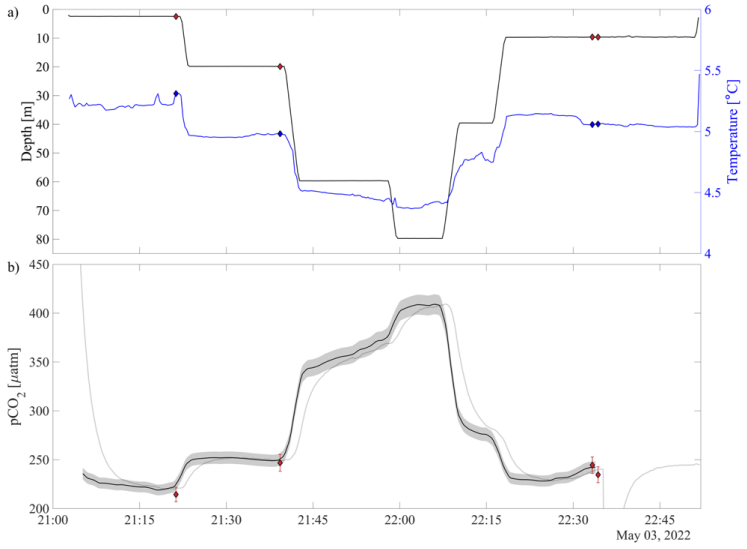

Figure 7. Profiling experiments from May 3rd with HydroC CO2T-0422-001 sensor mounted on the rosette. a) Pressure vs time on the left (black) axis with diamonds showing rosette CTD values of pressure (red filled), and temperature vs time on the right (blue) axis and temperature (blue filled) at the time of the bottle fire. b) pCO_2 measured by the rosette mounted SG HydroC CO_2 sensor as raw (gray line) and response time corrected signal (thick black line) with shaded relative uncertainty of 2.5% (weather goal; Newton et al., 2015). Discrete pCO_2 (pH_{lab}, DIC) shown as red diamonds with vertical red error bars showing combined standard uncertainty. Table 2 shows differences between discrete pCO_2 (pH_{lab}, DIC) and the HydroC pCO_2^{RTC} signal. The SG HydroC CO_2 sensor started a zeroing interval at 22:35 on May 3, 2022, so RTC pCO_2 is not shown after that time but signal recovery can be seen in the uncorrected signal (gray line).

https://doi.org/10.5194/egusphere-2024-1055
Preprint. Discussion started: 11 April 2024

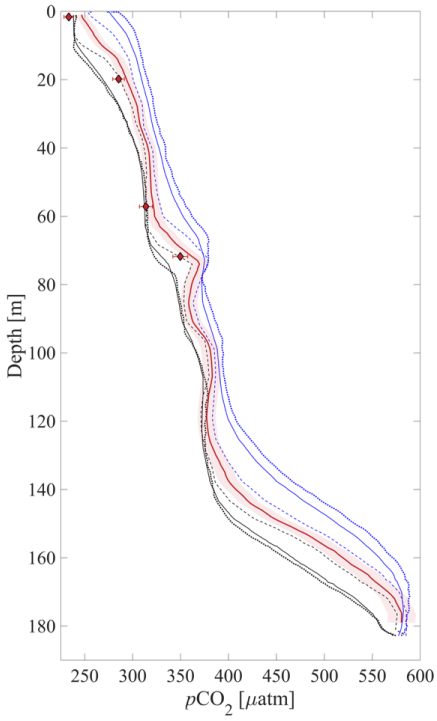

913

914 **Figure 8. CO_2 Seaglider data from a sea trial mission in spring 2022 in Resurrection Bay,**
915 **Seward, Alaska.** Depth profile of pCO_2 in µatm showing downcast (dotted black is the original
916 resolution, solid black is the 1 minute averaged downcast), upcast (dotted blue is the original
917 resolution, solid blue is the 1 minute averaged upcast), RTC pCO_2 following Dølven et al. (2022)
918 (dashed black line = downcast, dashed blue line = upcast) and 1-meter binned RTC profile (thick
919 red line) with shading showing the relative uncertainty of 2.5 %. Discrete pCO_2 (pH_{lab}, DIC)
920 shown as red diamonds with horizontal red error bars showing combined standard uncertainty
921 (Table 3).

922

https://doi.org/10.5194/egusphere-2024-1055
Preprint. Discussion started: 11 April 2024

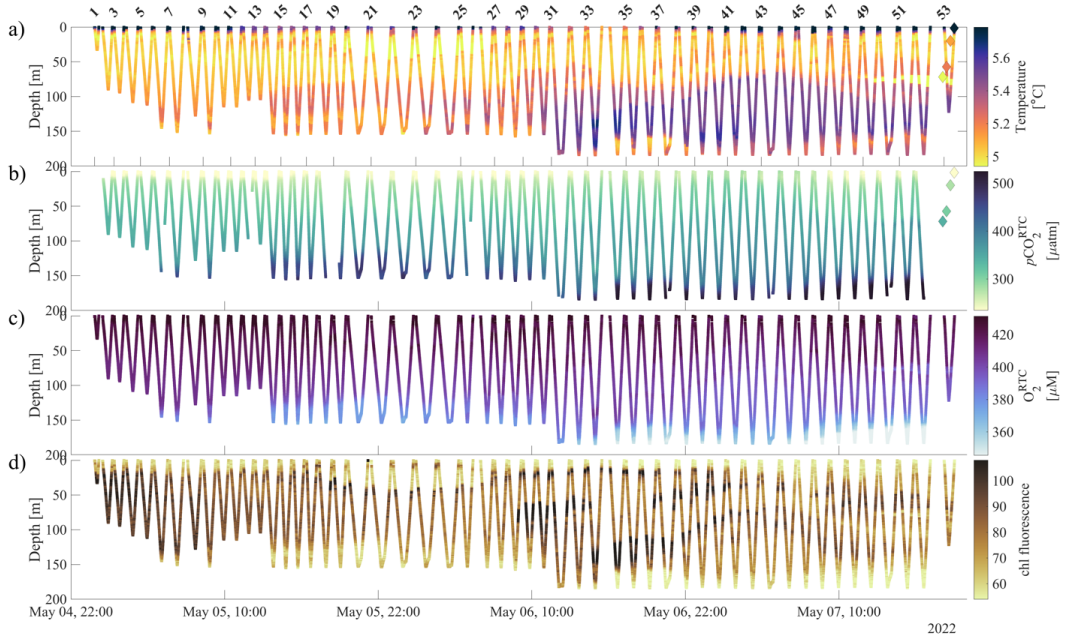

923

924 **Figure 9. CO_2 Seaglider data from a sea trial mission in spring 2022 in Resurrection Bay,**
925 **Seward, Alaska.** Depth profiles of a) Temperature [°C], b) RTC pCO_2 [µatm] c) RTC O_2 [µM],
926 and d) raw chlorophyll fluorescence. The triangles show discrete values that were taken during a
927 CTD cast (Table 3).

928

https://doi.org/10.5194/egusphere-2024-1055
Preprint. Discussion started: 11 April 2024

929

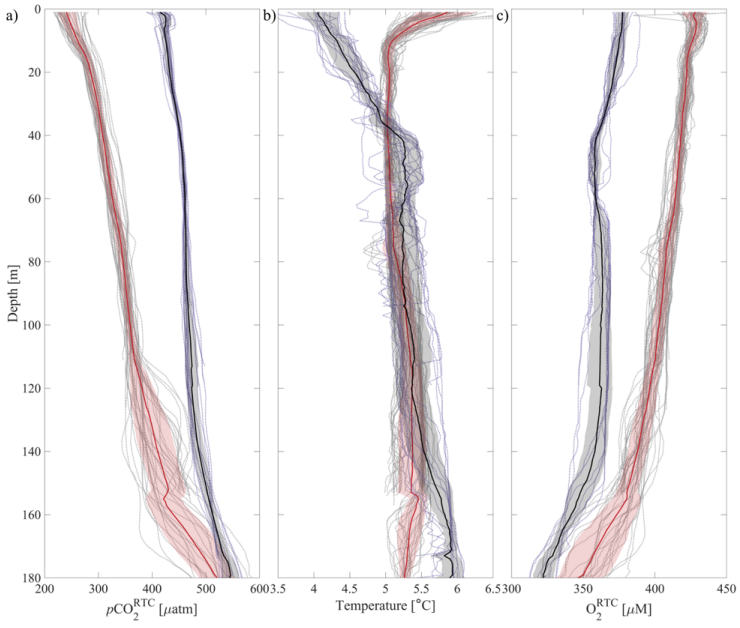

930

931 **Figure 10. Averaged CO_2 Seaglider profiles from May 2022 and February 2023 missions in**
932 **Resurrection Bay, Seward, Alaska.** Depth profiles of all 1-meter binned dives (dotted gray),
933 average 1-meter binned dive from May 2022 mission (red thick line, dive#1-53, May 5, 2022
934 00:01 to May, 7 2022 16:37) and February 2023 mission (black thick line, dive#1-17, February
935 8, 2023 20:50 to February 9, 2023 19:54) with shading showing the standard deviation of the
936 average. a) Response time corrected pCO_2 (pCO_2^{RTC}, µatm), b) temperature [°C], and c) response
937 time corrected oxygen (O_2^{RTC}, µM).

938

https://doi.org/10.5194/egusphere-2024-1055
Preprint. Discussion started: 11 April 2024

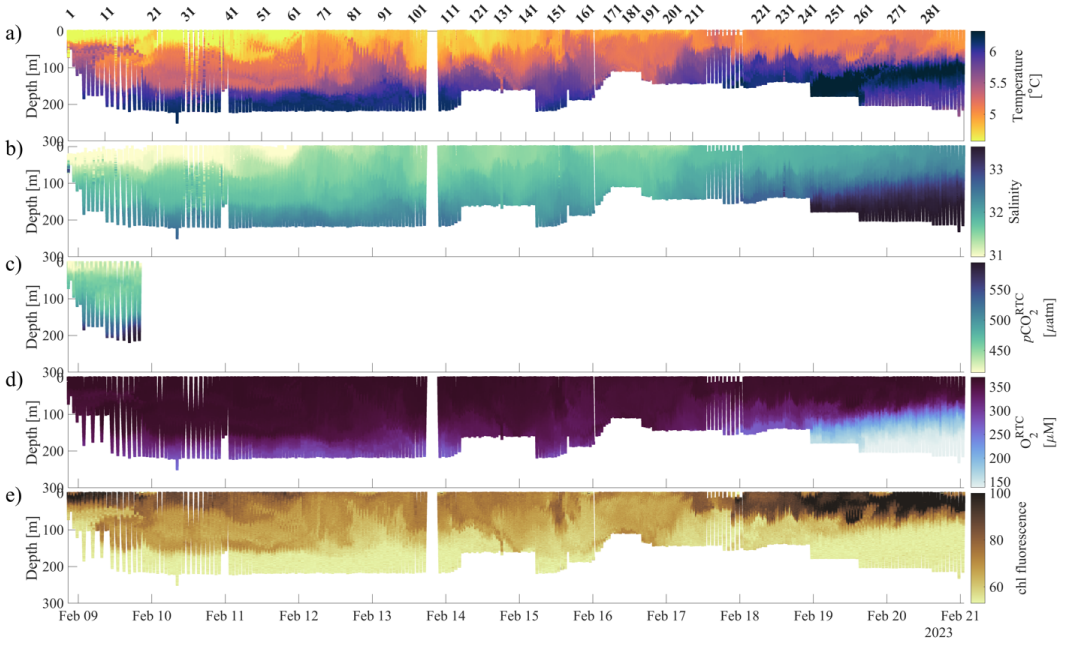

939

940 **Figure 11. CO_2 Seaglider data collected during the winter mission (February 8 - 20, 2023).**

941 Shown are a) temperature (°C), b) salinity, c) response time corrected pCO_2 (pCO_2^{RTC}, µatm), d)

942 response time corrected oxygen (O_2^{RTC}, µM), and e) raw chlorophyll fluorescence (chl

943 fluorescence) as time/dive number vs. pressure.

944

945

https://doi.org/10.5194/egusphere-2024-1055
Preprint. Discussion started: 11 April 2024

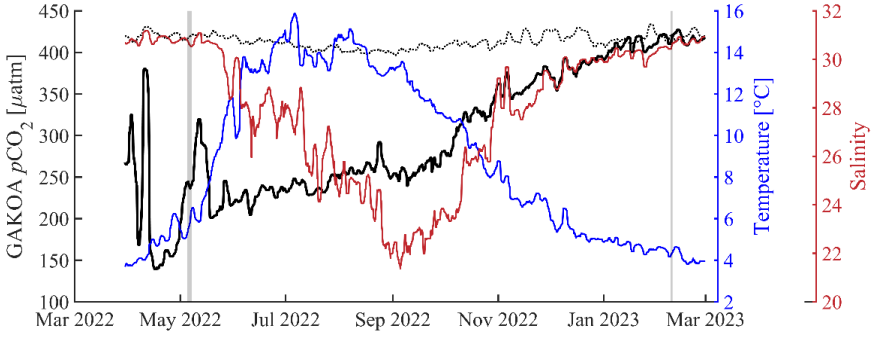

946

947 **Figure 12. National Oceanic Atmospheric Administration's Gulf of Alaska ocean**
948 **acidification surface time-series from March 2022 - 2023.** Left axis surface (dotted black line)
949 and air (black line, 4 meter above sea level) pCO_2 [uatm] and right axes sea surface temperature
950 (blue, °C) and sea surface salinity (red). All data shown as 3 day running mean. Vertical shaded
951 gray areas highlight the CO_2 Seaglider missions in May 2022 and February 2023. The mooring is
952 located at 59.911 °N, -149.35 °W (Monacci et al. 2023).

953

954

955

956